Acousto-Ultrasonic Evaluation Of Interlaminar Strength On CFRP Laminates

ACOUSTO-ULTRASONIC EVALUATION OF INTERLAMINAR STRENGTH ON CFRP LAMINATES

Claudia Barile[a,b], Caterina Casavola[a], Vincenzo Moramarco[a], Giovanni Pappalettera[a], Paramsamy Kannan Vimalathithan[a]

[a]*Dipartimento Meccanica, Matematica e Management, Politecnico di Bari, Viale Japigia 182, 70126 Bari, Italy*

[b]*IMAST S.c.a.r.l., Piazza Bovio 22, 80133 Napoli – Italy.*

Abstract

The acousto-ultrasonic approach is experimented on CFRP laminates. The test was organized in two modes: before the impact event and after the impact event; along longitudinal and transverse directions. Finally, the Compression after impact (CAI) test is performed on the impacted specimens to characterize its residual compressive strength. The AE descriptors loss along the longitudinal and transverse directions of the specimen are utilized to characterize the interlaminar strength of the specimen. With the help of Continuous Wavelet Transform (CWT) analysis, a hypothesis is created to discriminate the loss variation of AE descriptors to characterize the interlaminar strength of the material and the presence of damage or flaw in the material. The hypothesis holds true that the direction along which the relative loss of AE descriptors is low, has the lowest interlaminar strength. The mechanical results support the hypothesis created. With the proper channelling of acoustic signals and discrimination of data, the acousto-ultrasonic approach can be extended to characterize the interlaminar strength of the mechanical structures.

Keywords: Acoustic emission, drop weight impact, wavelet analysis, interlaminar strength, CFRP

Introduction

The developments in non-destructive evaluation (NDE) over the last three or four decades have provided us with enormous tools and techniques for structural monitoring and evaluation of materials. Most of the NDE techniques have proven successful in detecting flaws, assessing the effects of the flaws and other material anomalies. [1] The recent improvements in the evaluation tools have facilitated the full-field evaluation of

the size, location and the proximity of the flaws. The main purpose of the NDE is to monitor the health of a structure and assess its reliability in service. Although the advanced NDE tools are formidable in the health monitoring of the materials and structures, they sometimes fail to address the combined effects of minor flaws. [1,2] Composite materials have anomalies, which remain undetected during NDE, but affect the overall strength of the material. Such anomalies include poor bonding between the plies, the improper curing at the cohesive zone boundaries and the poor adhesion between the matrix and fibers. For instance, NDE can detect a void of size ranging from 0.01 mm in the matrix, however, the relevance of the presence of such void in determining the overall mechanical properties of the material remains debatable. On the other hand, the overall variation in mechanical properties of the material due to improper curing temperature and pressure cannot be addressed by NDE. [1-4]

The method that can address the relative strength and fracture resistance of the material is the acousto-ultrasonic approach. [1] The acousto-ultrasonic approach, as coined by A. Vary, utilizes the acoustic emission with ultrasonic sources. As quoted by the forerunner of this approach A. Vary, "It complements the other NDE approaches to material characterization and offers advantages to make it the preferred one to use in other cases". [1] It is quite clear from the statement that the acousto-ultrasonic approach does not disregard the necessity and utilization of the modern NDE tools but emphasizes on using this method in addressing the problems which cannot be resolved using conventional NDE techniques.

As the name implies, the method is based on simulating stress waves inside the material structure using an ultrasonic source. This approach utilizes the ultrasonic pulse source to convey stress waves inside the material. [5-7] The acousto-ultrasonic approach emphasises on characterizing the material medium through which the acoustic signals are transmitted rather than localizing the signal source. This is the major difference which makes the acousto-ultrasonic approach stand out from the conventional ultrasonic or acoustic emission techniques. [1,8]

Acoustic emission techniques study the transient waves produced in the material during the delamination, fiber breakage, matrix cracking or other phenomena under loading. [9] Characterizing the acoustic descriptors such as acoustic energy, peak amplitude, duration and counts of the received acoustic signal, the damage can be characterized. The different

acoustic energy and the peak amplitude of the received acoustic signals can be correlated to the different damage mechanisms responsible for the acoustic emission source. [5-7]

On the other hand, the acousto-ultrasonic approach is based on fact that the acoustic wave propagation is necessarily a parameter of material properties such as microstructure, morphology, porosity, bond quality, curing temperature and pressure and interlaminar properties. It means that, necessarily all the parameters that govern the damage mechanisms are the parameters that govern the acoustic wave propagation. [1,3,4,8]

There are contradicting reports: one suggesting the acoustic wave can propagate easily along the direction of the fiber and the other report suggesting the velocity of the acoustic waves are minimum along the direction of the fiber. [8,10] Despite the contradicting reports, there is a consensus about the acoustic waves: the acoustic waves are lamb waves in nature. [8-11] The reports have clearly explained the nature of the acoustic waves (which are the result of stress waves simulated in the material): the heterogeneity of the material results in the dispersion of the acoustic waves and the geometry and the material properties play a huge role in the propagation of the acoustic waves. [12-14]

In the recent years, the acoustic emission technique has been widely used to characterize the delamination behaviour, crack growth and crack localization in composite materials and civil structure. [15-18] The powerful evaluation tools, optimized algorithms and empirical models proposed by various researchers have revolutionised the application of acoustic emission technique. Nonetheless, while looking from the perspective of the acousto-ultrasonic approach, the propagation of the acoustic waves in an anisotropic material, the dispersion of acoustic waves through the different layers of the composite material and the influence of the interlaminar properties on the propagation of the acoustic waves is more significant while characterizing the delamination or other damage mechanisms in composites.

Thus, it becomes necessary to understand the propagation of acoustic wave before using the acoustic emission techniques to characterize the damage mechanisms. In the presented research work, the acousto-ultrasonic approach was tested in Compression After Impact (CAI) specimens. The presented work emphasis on characterizing the impact strength and CAI strength of the material using the acousto-ultrasonic approach.

Wavelet analysis was also performed on the simulated and received acoustic signals to characterize the waves in frequency-time domain.

Experimental Procedure

Materials

The composite used for the presented work is Carbon Fiber Reinforced Plastics (CFRP). The specimens were prepared using Resin Film Infusion (RFI) and stitching process. [19] The curing pressure was set at 1.5 bar at the temperature of 135 °C for 2h. Totally 5 specimens of dimensions 100 x 150 x 5 mm^3 were used. The specimen dimensions are as per ASTM D7136 - Standard Test Method for Measuring the Damage Resistance of a Fiber-Reinforced Polymer Matrix Composite to a Drop-Weight Impact Event. The details of the Fabric (F) and Tape (T) related to the layup and fiber orientation is as follows: $[45F/0T/0T/45F/0T/0T/0F/0T/0T/0F/0T/0T/45F/0T]_s$.

Methods

Acousto-Ultrasonic Test Procedure

The Auto-Sensor-Test (AST) module of PAC-PCI2 acoustic emission data acquisition system, supplied by MISTRAS, was used in this study. The AST module uses two or more piezoelectric sensors, which act as both the emitter and the receiver. Normally, the sensors are coupled to the surface of the specimen by a suitable couplant (silica grease). When the sensor crystals are excited by an external pulse, they send a pressure wave through the surface of the specimen. The first structural response of the pressure wave ricochets back from the surface of the specimen to the sensor. On the instance of receiving this first structural response, the pulsing sensor alters its role to a receiver. Then the receiver records the signals produced by the other sensors. An inbuilt algorithm allows recording the ricocheted signals at the structural border immediately as well as the signal emitted by the other sensor. Discriminating the difference between the structural response and the signal emitted by the other sensors can be achieved by properly setting the acquisition gate time. [20]

The test was conducted in two modes, along both the longitudinal direction and transverse direction of the specimen. The test was also performed on two occurrences:

before the impact event and after the impact event. The schematic of the testing mode is explained in Figure 1.

Figure 1. Schematic of Testing Modes

The reason behind testing the specimen along its two directions is to characterize the strength of the specimen along its two directions. Since the CFRP used in the study is orthotropic in nature, it is only suitable to characterize the strength of the specimen in both its direction. [21] For this purpose, the sensors are placed on the surface of the specimen, from the centre at a distance of 30 mm along the respective axes.

Two general purpose narrow band resonant sensors with high sensitivity (Model – R30α) were used in this study. The sensors were connected to the PAC data acquisition system through 2/4/6 AST amplifier with 20/40/60 gain. [22-24] However, the preamplifier gain was set at 40 dB and the band pass filter was set between 1 kHz and 3 kHz. Since the acoustic waves are simulated through the specimen, the sample length of the wave mostly lies between 2k and 4k. Thus, the sample length for the test was set at 3k. [13] The entire test was conducted at room temperature (~ 24 °C). The test was iterated for 5 times in both the direction for each specimen, before and after the impact event, respectively.

A pulse of 28 V spike (~100 dB bump) has been supplied to the piezoelectric sensors and the structural response was recorded and taken as the simulated acoustic signal. The width of the pulse is kept at 5 μs and 10 number of pulses were sent through the specimen with the interval of 100 ms between the consecutive pulses. The threshold for the receiving signals is kept at 35 dB. The acoustic emission (AE) descriptor such as, the peak amplitude, peak energy, duration and counts of the emitted and received signals are recorded. However, the peak amplitude was not considered in this study. [12, 20] It has been reported by the previous research works that the peak amplitude is mostly related with the signal transmitted over the surface of the specimen and it does not carry any significant information about the interlaminar property of the material. [12] This study emphasis on the interlaminar strength of the specimen, thus, the peak amplitude is overlooked in the discussion.

All the data were recorded, however, the average values of the 5 iterations were taken for the study purposes. The authors would like to add that the average values were taken for

the study since the standard deviation is relatively insignificant between the iterated results.

Drop Weight Impact Event

The drop weight impact test was conducted on INSTRON CEAST 9350 drop tower impactor. To create an out of plane impact event at 50 J energy, a drop mass of 2.781 kg with hemispherical striker tip of diameter 16 mm was dropped from the height of 1835.50 mm. The velocity of the impact 7.151 ms^{-1} creates an impact of 50 J energy to generate a Barely Visible Impact Damage (BVID) on the specimen. The impact event can be described as a small mass and low velocity impact (since the velocity of impact is below 15 ms^{-1}). [25]

When the impactor drops on the specimen, the specimen absorbs the energy. The peak force and energy absorbed by the specimen during the event are recorded. Then, the residual indentation produced by the impactor at the BVID location is measured using digital depth gauge. [26]

Compression after Impact (CAI) Test

The compression test was conducted for the impacted specimens in accordance with ASTM D7137 - Standard Test Method for Compressive Residual Strength Properties of Damaged Polymer Matrix Composite Plates. [27] The compression test was conducted in SCHENK servo hydraulic testing machine (250 kN load capacity) at a crosshead movement of 1.25 $mm\,min^{-1}$. The fixture used is as recommended by ASTM D7137, supporting upper and lower edges of the specimen and also holding the specimen rigidly on its sides (Figure 2).

Figure 2 – Fixture and setup for Compression After Impact (CAI) test

Results

Acousto-Ultrasonic Results – Before Impact Event

Five specimens were taken for this acousto-ultrasonic study. The acoustic emission descriptors (Peak Amplitude, Acoustic Energy and Duration) of the sent and received signals before the impact event are recorded. As mentioned in the previous section

(Figure 1), the test was conducted separately along the longitudinal and transverse directions. The recorded AE descriptors are provided in Table 1 and Table 2.

Table 1 – AE descriptors along longitudinal direction before the impact event

Table 2 – AE descriptors along transverse direction before the impact event

The relative loss (in percentage) between the sent and received AE descriptors along both the directions are presented in Figure 3.

Figure 3 – AE descriptor loss in percentage along longitudinal and transverse directions before the impact event

Drop Weight Impact and CAI Results

Results of the drop weight impact test are provided in this section before discussing the results of the AE descriptors after the impact event. All the five specimens were subjected to the drop weight impact test to create the BVID. The force and energy absorbed by the specimen were recorded and the plot between the force and the time of impact are provided in Figure 4. The residual indentation of the BVID was measured; the peak energy and peak force absorbed by the specimen during the impact event was recorded and presented in Table 3. The compression after impact results were also included in Table 3, while the plot between the compression load applied to the crosshead displacement has been provided in Figure 5.

Figure 4 – Force vs Time of impact plot for all specimens during out of plane impact test

Table 3 – BVID residual indentation, Drop Weight Impact Test and CAI Test Results

Figure 5 – Compression after Impact Load vs Displacement

Acousto-Ultrasonic Results – After Impact Event

Following the impact test, the specimens were tested again using the acousto-ultrasonic approach to characterize the changes in the AE descriptors value. The recorded AE

descriptors along the longitudinal and transverse direction are provided in Table 4 and Table 5, respectively.

Table 4 – AE descriptors along longitudinal direction after impact event

Table 5 – AE descriptors along transverse direction after impact event

Similar to the previous instance, the relative loss in the AE descriptors between the signal sent and received are presented in Figure 6.

Figure 6 – AE descriptor loss in percentage along longitudinal and transverse directions after the impact event

The wavelet analysis was performed for the AE signals simulated to all the specimens. The simulated signal corresponds to the AE signal produced by the 100 dB bump in all the cases. Consequently, the AE signal sent are all similar and has the same waveform. The wavelet analysis of signal sent is provided in Figure 7. The wavelet analysis was performed in continuous wavelet analysis (CWT) module, since it is appropriate for studying the wavelet in time-frequency domain. [28] The analytical Morlet wavelet was used for characterizing the wavelets. The number of octaves for the analysis was set as 3 and the voices per octave as 32.

Figure 7 – CWT wavelet of AE signal sent

The CWT wavelet of signals received along the longitudinal and transverse directions, before impact, are produced in Figure 8 and Figure 9, respectively. In the similar way, the CWT wavelet of signals received along the longitudinal and transverse directions, after impact, is presented in Figure 10 and Figure 11, respectively.

Figure 8 – CWT Wavelet of signals received along Longitudinal Direction before Impact

Figure 9 – CWT Wavelet of signals received along Transverse Direction before Impact

Figure 10 – CWT Wavelet of signals received along Longitudinal Direction after Impact

Figure 11 – CWT Wavelet of signals received along Transverse Direction after Impact

The results obtained from the acousto-ultrasonic approach can be used to characterize the material in two different ways. From the variation in AE descriptors and their relative loss along the longitudinal and transverse directions, the strength of the material along the respective directions can be predicted. From the wavelet analysis, it is possible to characterize the extent of interlaminar damage in the specimen after the drop weight impact.

Discussion

Despite the acoustic signal sent through the specimens correspond to the 28 V spike/100 dB bump, the acoustic energy and duration of the input signal vary between the different specimens (Table 1 and Table 2). The thickness of the couplant through with the sensors are contacted to the surface of the specimen affects the input acoustic signal. It has been reported previously that both the thickness of couplant and holding pressure of the sensor affects the input acoustic signals, however, in an insignificant way. [11] Thus, it can be deemed as not relevant for the scope of this work. This is the reason why the relative loss in the AE descriptors between the sent and received signals are taken for the discussion.

The AE descriptors of sent and received signals along longitudinal and transverse directions are provided in Table 1 and Table 2, respectively. The relative loss between the signals are provided in Figure 3. The first major question that arises while looking at the results is, why the relative loss in amplitude is very much lower when compared to the other AE descriptors? The peak amplitude represents the signal which is transmitted along the surface of the specimen rather than through its interlaminar structure. The peak amplitude neither does correspond to the structural response of the specimen nor does carry any information about the interlaminar properties of the specimen. It has been recommended to consider the AE energy rather than the peak amplitude.

The second important observation is the differences between the AE descriptors along longitudinal and transverse directions. In specimen AU1, along the longitudinal direction, the relative loss of AE energy is 93.5%, while it is 79.71% along the transverse direction. Similarly, in all the other specimens the relative loss in AE energy and duration along

longitudinal direction is more than the transverse direction. This result, when compared with the specimens after the drop weight impact, becomes even more intriguing (Figure 12).

Figure 12 – Top and Bottom surface of the specimen after Drop Weight and CAI tests

After the drop weight event, the specimen is measured for the BVID. It can be observed that a residual indentation is formed on the top surface of specimen; while the impact energy has transmitted through the surface and severe damage can be seen at the bottom surface. In all the specimens, the fibers along the transverse direction has been broken by the impact. Although the extent of interlaminar damage cannot be observed through visual inspection, it can be explained through the results obtained.

After the drop weight event, the fibers in the transverse direction have broken. This shows that the drop weight impact energy did not transmit symmetrically through the specimen. The fiber breakage in the transverse direction represents that the interlaminar strength along the transverse direction is low and it is responsible for the fiber breakage along that specific direction.

The phase direction of the material along which the interlaminar strength is low also has the lowest acoustic energy (Figure 3). Supposedly, an assumption can be made to understand the relation between the structural response and the acoustic signal transmission. The phase direction of the material which has the lowest interlaminar strength permits the easy propagation of the acoustic signal. This maybe the reason why the AE descriptor loss along the transverse direction is less than the longitudinal direction.

However, this is just an assumption made. To verify the credibility of the assumption made, the AE descriptor loss along the transverse direction in different materials is compared with the mechanical experimental results.

After the drop weight impact, the residual indentation of all the specimens were measured using digital depth gauge. The specimen AU1 and AU5 have the residual indentation of -0.59 mm and -1.74 mm, respectively, which is by far more when compared to the other specimens. The peak force absorbed by AU1 and AU5 are 9849.16 N and

9090.62 N, respectively. The peak force and energy absorbed by the aforementioned specimens are also very low when compared with AU2, AU3 and AU4 (Table 3). In the similar way, after the compression test, the specimens AU1 and AU5 also have the lowest CAI force and CAI strength. Now, this clearly shows that the interlaminar integrity of the material AU1 and AU5 is comparatively lower than the other specimens. AU1 and AU5 have the highest residual indentation and absorbed low impact energy and have shown poor CAI strength.

Considering the relative loss of AE in transverse direction (Figure 3) between the different specimens, AU1 and AU5 have the lowest AE energy loss (79.71% and 81.01%, respectively) when compared to the other specimens. Expectedly, these two specimens have the lowest mechanical properties (interlaminar properties). The assumption initially made for understanding the relation between the AE descriptors and the interlaminar property of the material seems to hold true.

A general hypothesis can be created following these observations. The direction along which the AE descriptor loss is low, has the lowest interlaminar strength. The hypothesis can be verified by comparing the results from Figure 3 and the experimental drop weight impact and CAI results from Table 3. Figure 4 also shows the lowest energy absorbed by AU5 during the drop weight impact event. Although AU1 seems to follow the same Force vs Time curve as the other specimens, the peak force and energy absorbed by AU1 is also very low. If this hypothesis holds true, the interlaminar strength of the material can be characterized by the acousto-ultrasonic approach.

However, to verify this hypothesis more elaborately, the acousto-ultrasonic approach was tested on the specimens after the drop weight impact event and the results are presented in Table 4 and Table 5. Similar to the previous instant, the relative loss between the AE descriptors are also provided in Figure 5. From the results, it can be noted that the relative loss of AE energy along both the longitudinal and transverse directions are quite higher (average loss of 95%). Along the longitudinal direction, the specimen AU1 and AU5 experienced the maximum loss (97.91% and 97.37%, respectively); in transverse directions as well the same AU1 and AU5 have experienced the maximum loss. The transmission medium of the acoustic signal was disrupted by the fiber breakage along the transverse direction. This results in the loss of acoustic energy in transverse direction to increase from 79.71% to 96.14% in AU1, before and after impact and 81.01% to 96.45%

in AU5. Similarly, the same increase in AE loss can be observed in all the specimens between before impact and after impact event.

This contradicts the hypothesis that the lower AE descriptor loss represents the lowest interlaminar strength of the material. This contradiction can be rectified by performing wavelet analysis (CWT) of the AE signals in Time-Frequency domain. The continuous wavelet analysis was performed for all AE signals, both before and after impact in the signals tested from longitudinal and transverse direction.

The CWT wavelet of the input signal has been presented in Figure 7. Since the input signal corresponds to the 100 dB bump, the frequency domain can be seen at a magnitude of 10 at the normalized frequency 0.3 to 0.35 region. This wavelet can be taken as the reference to compare the received signals.

The CWT wavelets of the signals received along longitudinal direction, before impact, (Figure 8) has the maximum magnitude of 1.6 in the 0.3 to 0.35 normalized frequency region. Unlike the input signal, the received signals are modulated over longer time intervals. Moreover, the wavelet can be seen in two distinguishable frequency domains, one being above 0.25 normalized frequency and the other one, between 0.1 and 0.25 frequency domain. The two distinguishable frequency domains can represent the acoustic wave propagated through the fiber and the polymer matrix, respectively. A similar two frequency domains were observed in the previous study on the acoustic wave propagation in CFRP. [12]

Upon looking at the CWT wavelet of received signals along transverse direction before the impact event, (Figure 9), the signals are modulated over shorter time intervals compared to the signals along longitudinal direction. Moreover, the maximum magnitude of the received signals are 2.5 for specimen AU1 and around 2.2 for rest of the specimens. These CWT results also show the wavelets in two distinguishable frequency domain much like in Figure 8. Thus, it is safe to say that the two distinguishable frequency domains represent the AE signal propagated in different phases of the material.

However, while examining the CWT results of the signals received along longitudinal direction after the impact event, except for specimen AU5, all the other specimens exhibit one frequency domain (Figure 10). The maximum magnitude of the normalized frequency is merely 0.45 when compared to 1.6 in the CWT before impact. On the

contrary side, the CWT along the transverse direction shows two frequency domains (Figure 11). It can also be noted that the maximum magnitude is 0.7, for specimen AU3 and for the rest of the specimens, it is around 0.5.

This shows that, despite the relative loss in AE has been more in the specimens after impact, the magnitude of the CWT wavelet can be used to identify whether the high relative loss represents the lower interlaminar strength or the damage/flaw in the material. The extent of interlaminar damage can also be explained by the CWT analysis, nonetheless, the scope for that is in the future.

Thus, a conditional hypothesis can be created to analyse the interlaminar strength of the material using the acousto-ultrasonic approach. The lower the relative loss in AE descriptors along a specific direction represents the lower interlaminar strength of the material in the same direction. At the same time, the wavelet analysis must be performed to support this hypothesis. The magnitude of the frequency can be used to discriminate whether the relative loss of the acoustic energy represents the interlaminar strength of the material or the presence of serious flaws or damages.

These observations have opened the questions whether the presence of flaw can be detected using the wavelet analysis and whether it is possible to estimate the interlaminar strength of the material with the acousto-ultrasonic approach. The scope for expanding the acousto-ultrasonic approach using a series of piezoelectric sensors assembled in different patterns and orientations will provide more details about the interlaminar integrity of the material.

Conclusion

The acousto-ultrasonic approach was tested for CFRP specimens subjected to low velocity drop weight impact. The specimen was tested along both its longitudinal and transverse axes, before and after the drop weight impact event. Compression after impact test was also performed on the specimen to characterize its strength with the presence of BVID. The acousto-ultrasonic results were used to characterize the interlaminar strength of the material along both the longitudinal and transverse directions. A conditional hypothesis was made to evaluate the results: the direction along which the relative loss of AE descriptors is low, possess the lower interlaminar strength. With the aid of wavelet analysis, it is possible to discriminate the lower interlaminar strength and

the presence of damage/flaw in the material. Using the acousto-ultrasonic approach, it seems relatively easy to characterize the material properties. Along with the proper evaluation tools and techniques, this approach has a greater scope in discriminating the types of defects and the position of the flaws in the material.

Acknowledgement

The authors thank the Regional Apulia Call "Support for Regional Technological Cluster for Innovation" for financial support, specifically COGEA – Composite Certification in General Aviation (OES4AM4).

References

1. Vary A. The Acousto-Ultrasonic Approach. In: Duke J.C. (eds) Acousto-Ultrasonics. Springer, Boston, MA, 1988.
2. Kanninen MF, Popelar CH. Advanced Fracture Mechanics. Oxford University Press, New York, 1985.
3. Vary A. A Review of Issues and Strategies in Nondestructive Evaluation of Fiber Reinforced Structural Composites. In: "New Horizons -Materials and Processes for the Eighties," SAMPE, Azusa, 1979.
4. Vary A, Bowles KJ. An Ultrasonic-Acoustic Technique for Nondestructive Evaluation of Fiber Composite Quality. Polymer Engineering and Science 1979;19:373-376.
5. Marec A, Thomasa JH, El Guerjouma R. Damage characterization of polymer-based composite materials: multivariable analysis and wavelet transform for clustering acoustic emission data. Mechanical Systems and Signal Processing 2008;22:1441–1464.
6. Davijani AAB, Hajikhani M, Ahmadi M. Acoustic emission based on sentry function to monitor the initiation of delamination in composite materials. Materials & Design 2011;32:3059–3065.

7. Ativitavas N, Fowler T, Pothisiri T. Acoustic emission characteristics of pultruded fiber reinforced plastics under uniaxial tensile stress. In: Proceedings of European WG on AE, Berlin; 2004. p. 447–54.

8. Vary A. Acousto-ultrasonic characterisation of fiber reinforced composites. Materials Evaluation 1982;40:650–654.

9. Barile, C., Casavola, C., Pappalettera, G., Pappalettere, C. Acoustic emission analysis of aluminum specimen subjected to laser annealing. Conference Proceedings of the Society for Experimental Mechanics Series, 8, pp. 309-315, 2014.

10. Moon SM, Jerina KL, Hahn HT. Acousto-Ultrasonic Wave Propagation in Composite Laminates. In: Duke J.C. (eds) Acousto-Ultrasonics. Springer, Boston, MA, 1988.

11. Pollard HF. Sound Waves in Solids. Pion Limited, London, 1977.

12. Finkel P, Mitchell JR, Carlos MF. Experimental study of 'Auto Sensor Test-Self Test Mode' for acoustic emission system performance verification. AIP Conference Proceedings 2000;509:1995–2002.

13. Barile C, Casavola C, Pappalettera G, Vimalathithan PK. Experimental wavelet analysis of acoustic emission signal propagation in CFRP. Engineering Fracture Mechanics 2018, https://doi.org/10.1016/j.engfracmech.2018.05.030

14. Kautz HE. Ray Propagation Path Analysis of Acousto-Ultrasonic Signals in Composites. In: Duke J.C. (eds) Acousto-Ultrasonics. Springer, Boston, MA, 1988.

15. Oskouei AR, Zucchelli A, Ahmadi M, Minak G. An integrated approach based on acoustic emission and mechanical information to evaluate the delamination fracture toughness at mode I in composite laminate. Materials & Design 2011;32:1444–1455.

16. Romhany G, Szebényi G. Interlaminar fatigue crack growth behavior of MWCNT/carbon fiber reinforced hybrid composites monitored via newly developed acoustic emission method. Express Polymer Letters 2012;6:572–580.

17. Ohtsu M. The history and development of acoustic emission in concrete engineering. Magazine of Concrete Research 1996;48:321–330.

18. Pollock AA. Acoustic emission-2: acoustic emission amplitudes. Non-Destructive Testing 1973;6:264–269

19. Barile C, Casavola C. Mechanical characterization of carbon fiber reinforced plastics specimens for aerospace applications. Polymer Composites 2018, https://doi.org/10.1002/pc.24723

20. PCI-2 based AE Systems. Associated with AEWIN for PCI – 2 software. Princeton Junction (NJ): Physical Acoustics Corporation [Chapter 6] <www.mistrasgroup.com>.

21. Casavola, C., Palano, F., De Cillis, F., Tati, A., Terzi, R., Luprano, V. Analysis of CFRP joints by means of T-pull mechanical test and ultrasonic defects detection. Materials, 11 (4), art. no. 620, 2018.

22. Barile C, Casavola C, Pappalettera G. Acoustic emission waveform analysis in CFRP under Mode I test. Engineering Fracture Mechanics 2018, https://doi.org/10.1016/j.engfracmech.2018.05.030

23. Barile C. Innovative mechanical characterization of CFRP using acoustic emission technique. Engineering Fracture Mechanics 2018, https://doi.org/10.1016/j.engfracmech.2018.02.024

24. Barile, C., Casavola, C. Fracture behavior of unidirectional composites analyzed by acoustic emissions technique. Conference Proceedings of the Society for Experimental Mechanics Series, 7, pp. 121-127, 2018

25. Sebaey TA, González EV, Lopes CS, Blanco N, Costa J. Damage resistance and damage tolerance of dispersed CFRP laminates: Design and optimization. Composite Structures 2013;95:569-576.

26. ASTM D7136 / D7136M-15, Standard Test Method for Measuring the Damage Resistance of a Fiber-Reinforced Polymer Matrix Composite to a Drop-Weight Impact Event, ASTM International, West Conshohocken, PA, 2015, www.astm.org

27. ASTM D7137 / D7137M-17, Standard Test Method for Compressive Residual Strength Properties of Damaged Polymer Matrix Composite Plates, ASTM International, West Conshohocken, PA, 2017, www.astm.org

28. Understanding Wavelets. Part 4: An Example application of Continuous Wavelet Transform. From the series: Understanding Wavelets www.mathworks.com 2016.

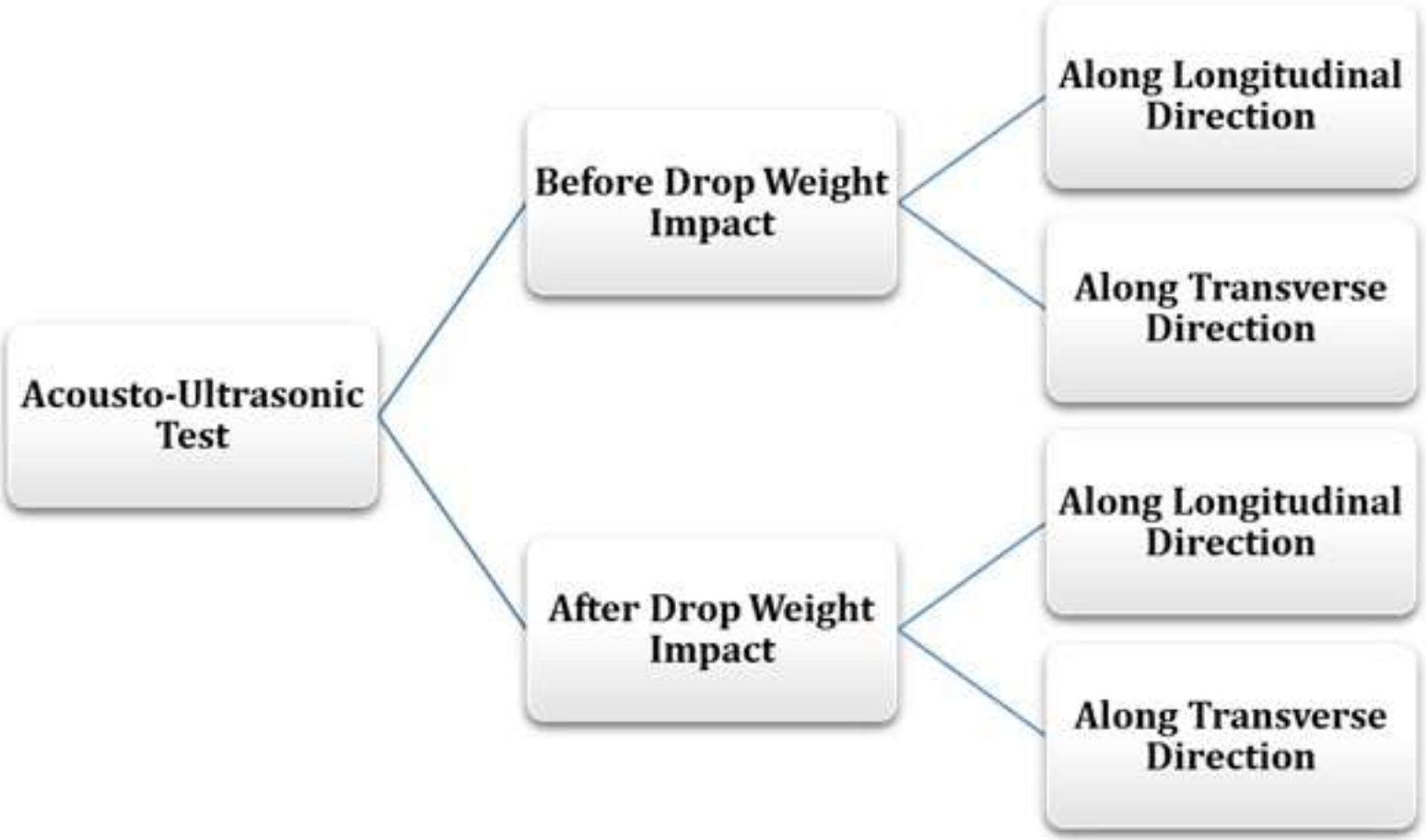
Acousto-Ultrasonic Test
Before Drop Weight Impact
After Drop Weight Impact
Along Longitudinal Direction
Along Transverse Direction
Along Longitudinal Direction
Along Transverse Direction

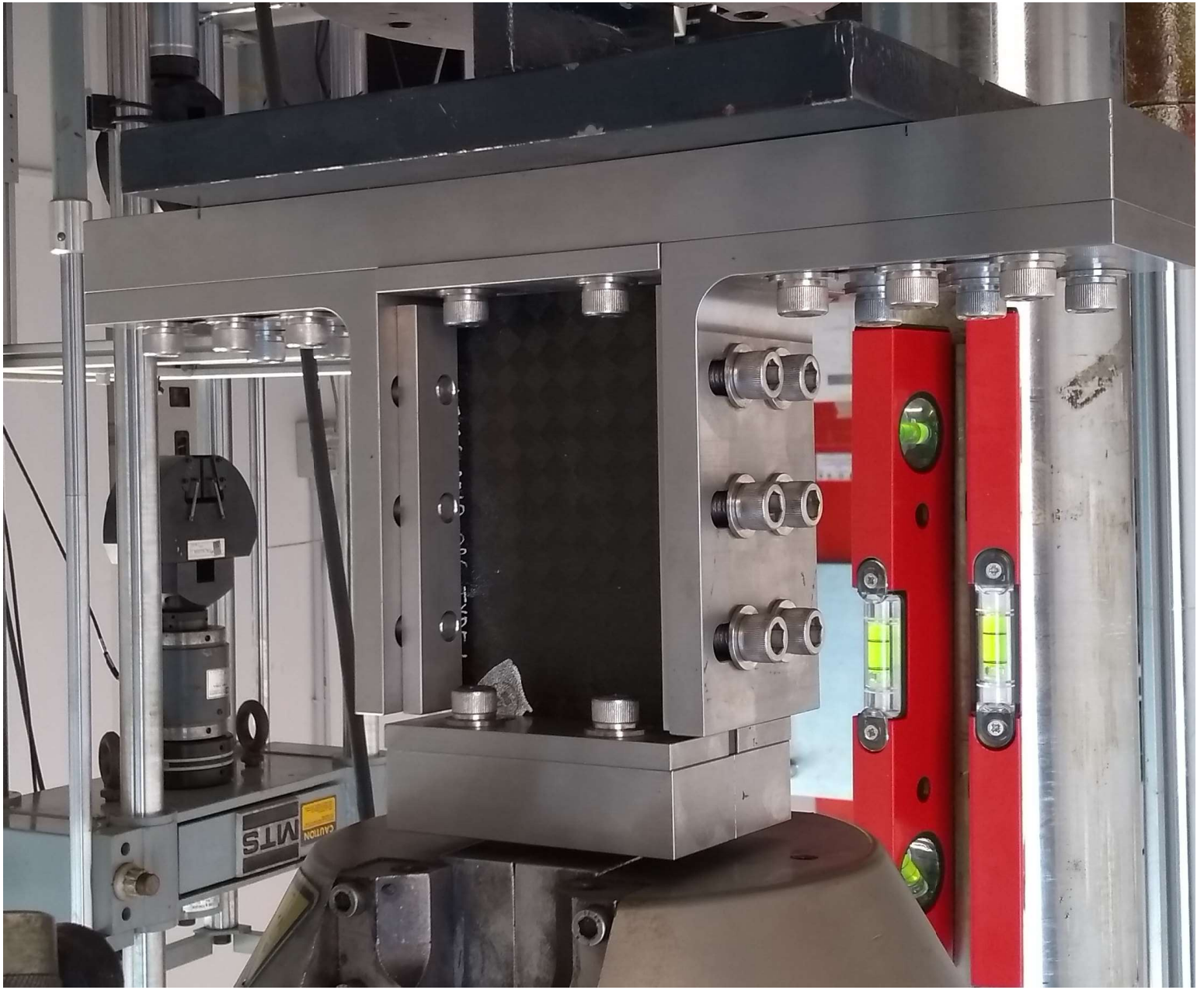
MTS
CAUTION

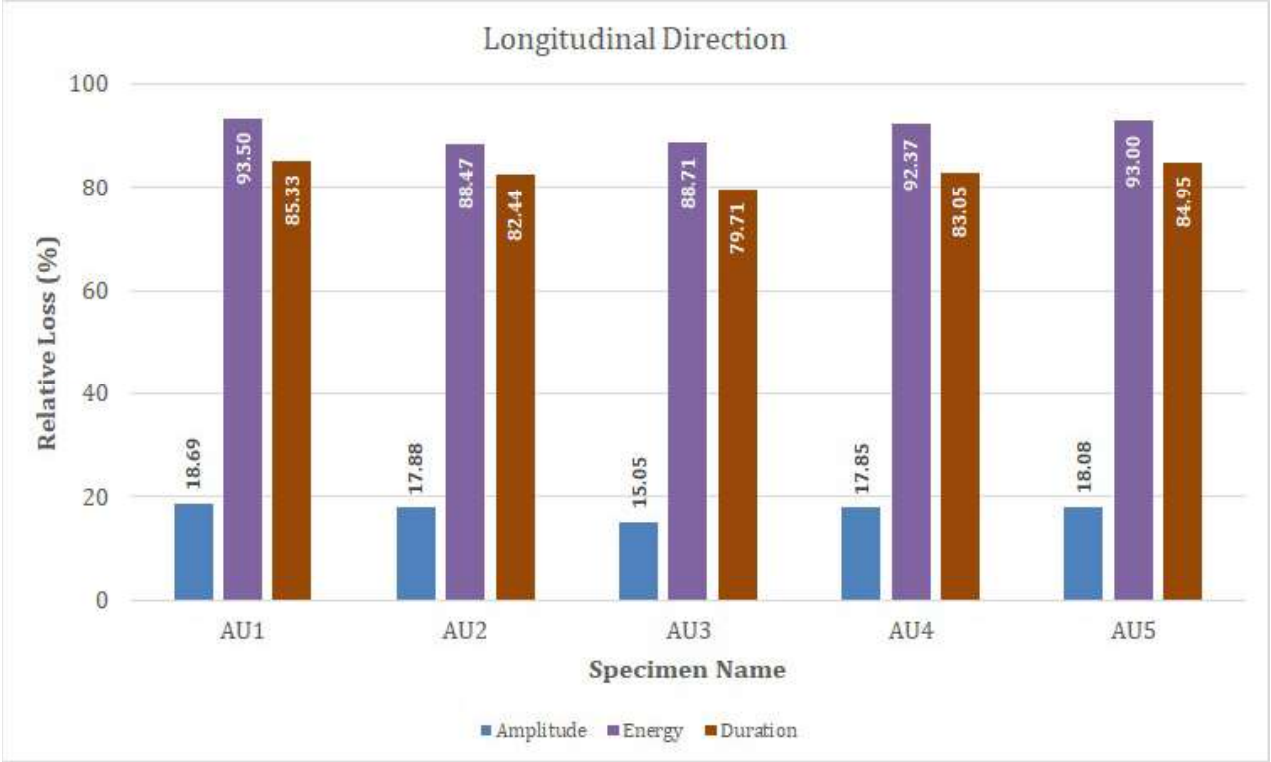
Longitudinal Direction
Relative Loss (%)
100
80
60
40
20
0
18.69
93.50
85.33
17.88
88.47
82.44
15.05
88.71
79.71
17.85
92.37
83.05
18.08
93.00
84.95
AU1
AU2
AU3
AU4
AU5
Specimen Name
Amplitude
Energy
Duration


Transverse Direction
Relative Loss (%)
100
80
60
40
20
0
10.61
79.71
75.94
12.73
84.44
78.12
11.92
85.17
78.02
13.64
89.34
81.23
12.63
81.01
76.41
AU1
AU2
AU3
AU4
AU5
Specimen Name
Amplitude
Energy
Duration

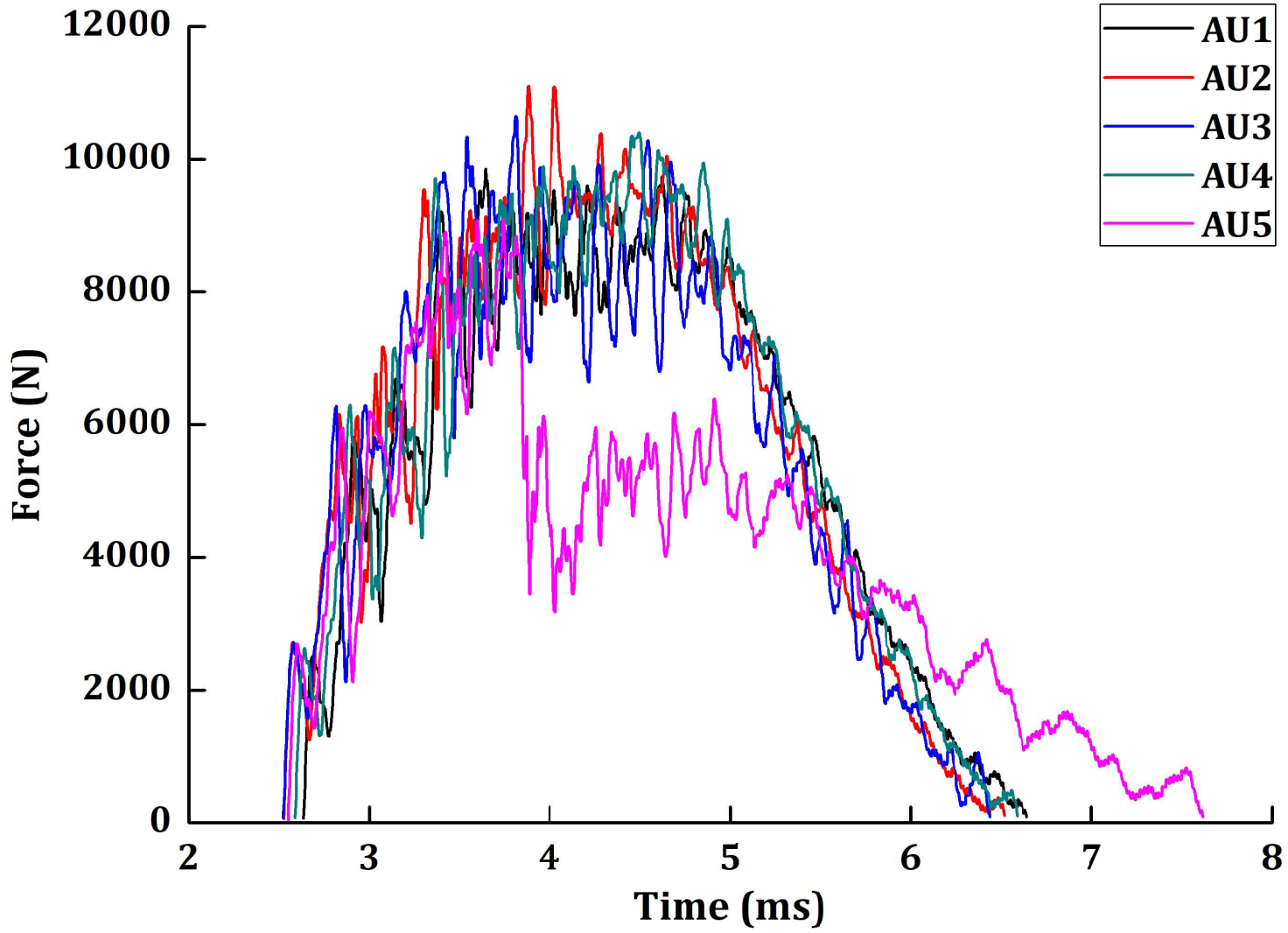
12000
10000
8000
6000
4000
2000
0
Force (N)
2
3
4
5
6
7
8
Time (ms)
AU1
AU2
AU3
AU4
AU5

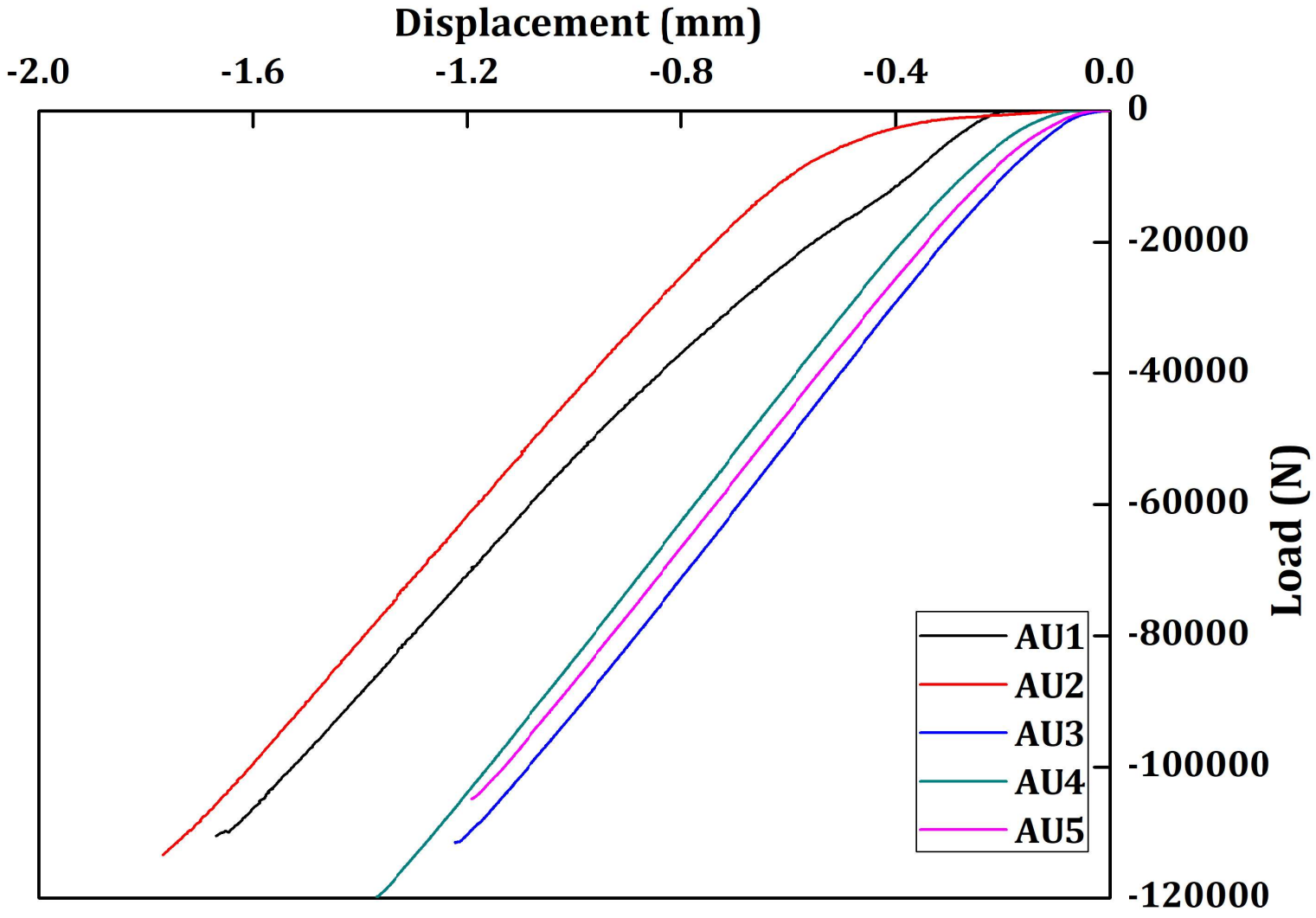
Displacement (mm)
-2.0
-1.6
-1.2
-0.8
-0.4
0.0
0
-20000
-40000
-60000
-80000
-100000
-120000
Load (N)
AU1
AU2
AU3
AU4
AU5


Longitudinal Direction
Relative Loss (%)
100
80
60
40
20
0
28.28
97.91
92.49
20.10
95.11
92.60
26.64
97.24
91.96
27.07
97.21
92.15
28.38
97.37
91.82
AU1
AU2
AU3
AU4
AU5
Specimen Name
Amplitude
Energy
Duration


Transverse Direction
Relative Loss (%)
100
80
60
40
20
0
25.76
96.14
89.28
24.24
94.77
85.28
22.22
87.65
90.05
24.49
94.64
87.33
28.69
96.45
91.96
AU1
AU2
AU3
AU4
AU5
Specimen Name
Amplitude
Energy
Duration

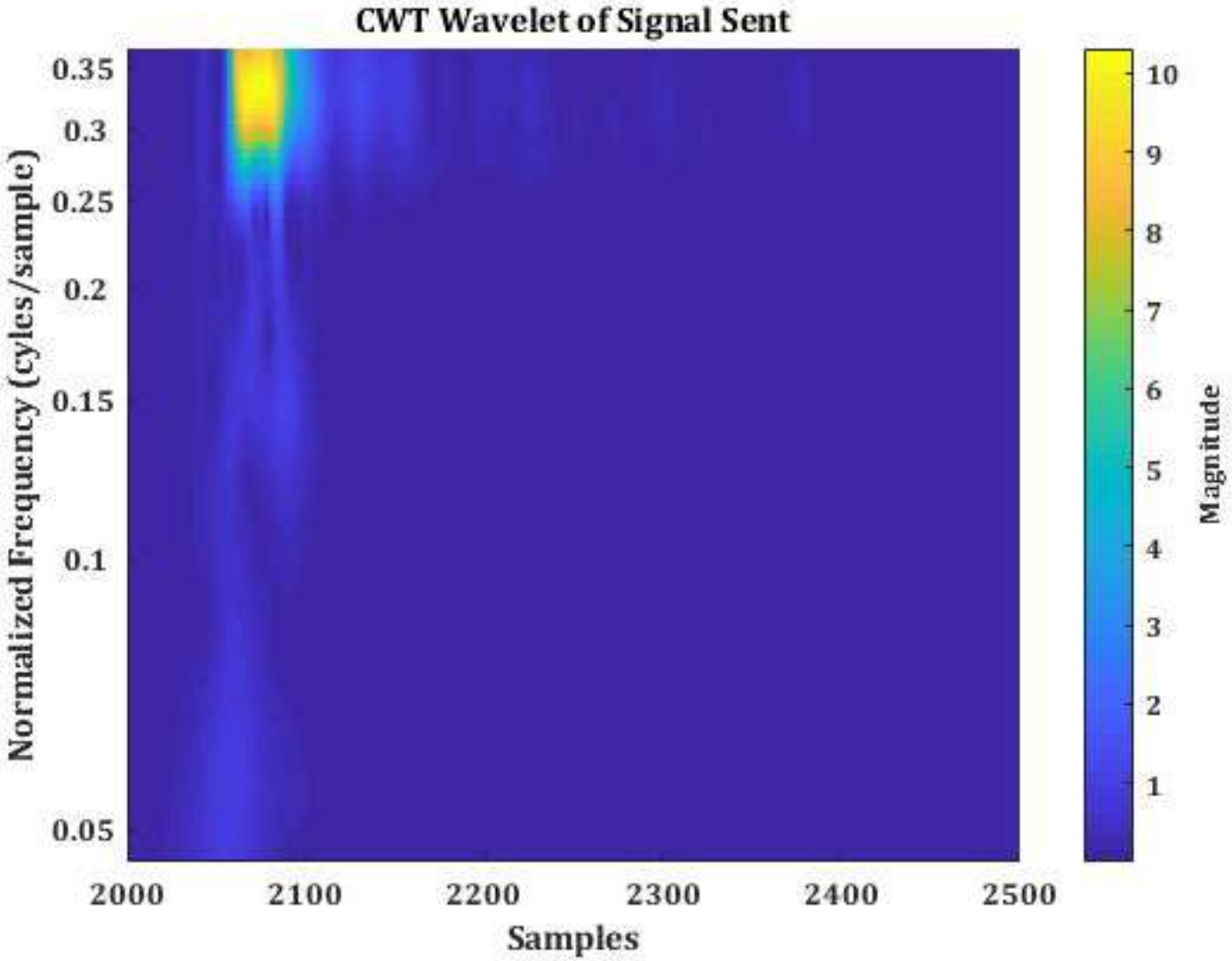
CWT Wavelet of Signal Sent
Normalized Frequency (cyles/sample)
0.35
0.3
0.25
0.2
0.15
0.1
0.05
2000
2100
2200
2300
2400
2500
Samples
Magnitude
10
9
8
7
6
5
4
3
2
1

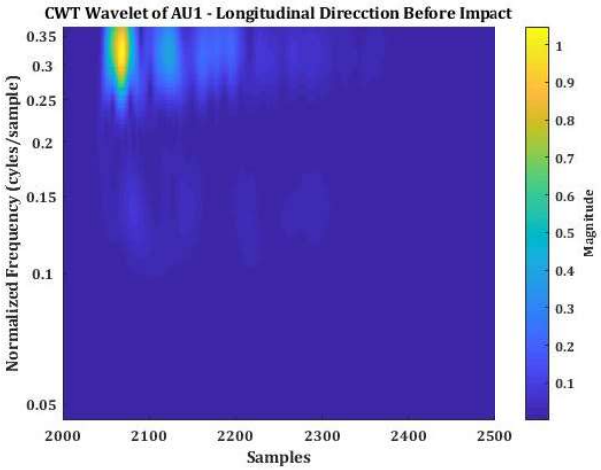
CWT Wavelet of AU1 - Longitudinal Direcction Before Impact
Normalized Frequency (cyles/sample)
0.35
0.3
0.25
0.2
0.15
0.1
0.05
2000
2100
2200
2300
2400
2500
Samples
Magnitude
1
0.9
0.8
0.7
0.6
0.5
0.4
0.3
0.2
0.1

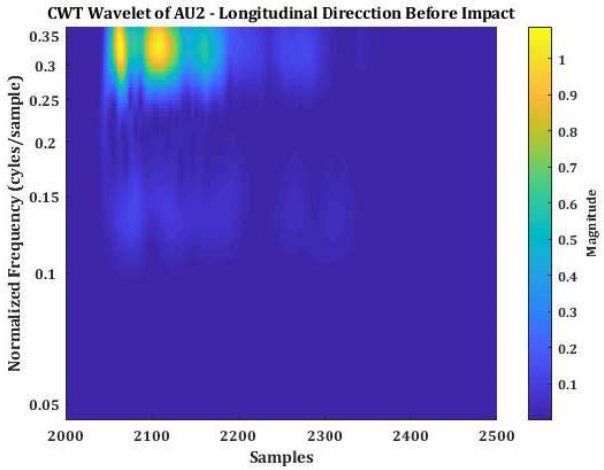
CWT Wavelet of AU2 - Longitudinal Direcction Before Impact
Normalized Frequency (cyles/sample)
0.35
0.3
0.25
0.2
0.15
0.1
0.05
2000
2100
2200
2300
2400
2500
Samples
Magnitude
1
0.9
0.8
0.7
0.6
0.5
0.4
0.3
0.2
0.1

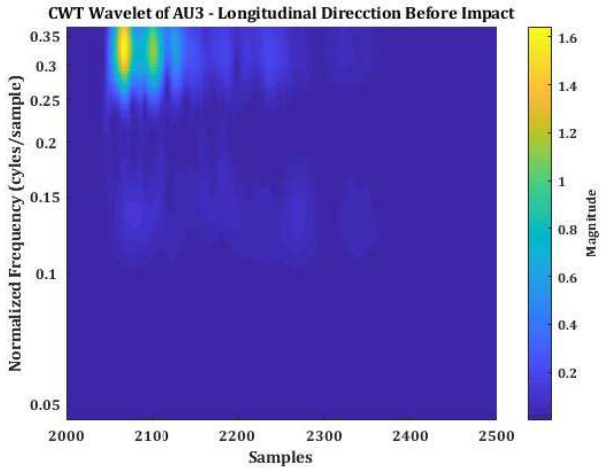
CWT Wavelet of AU3 - Longitudinal Direcction Before Impact
Normalized Frequency (cyles/sample)
0.35
0.3
0.25
0.2
0.15
0.1
0.05
2000
2100
2200
2300
2400
2500
Samples
Magnitude
1.6
1.4
1.2
1
0.8
0.6
0.4
0.2

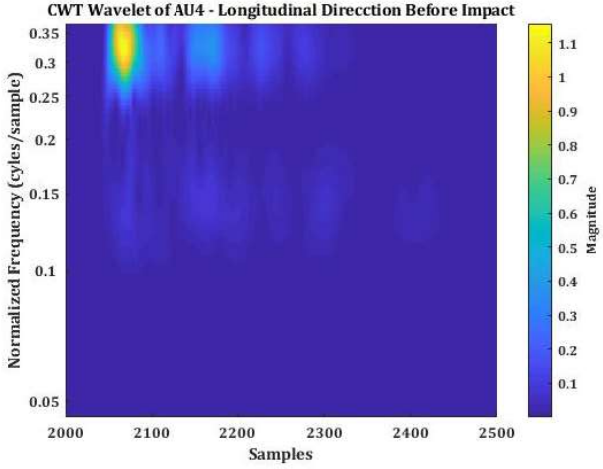
CWT Wavelet of AU4 - Longitudinal Direcction Before Impact
Normalized Frequency (cyles/sample)
0.35
0.3
0.25
0.2
0.15
0.1
0.05
2000
2100
2200
2300
2400
2500
Samples
Magnitude
1.1
1
0.9
0.8
0.7
0.6
0.5
0.4
0.3
0.2
0.1

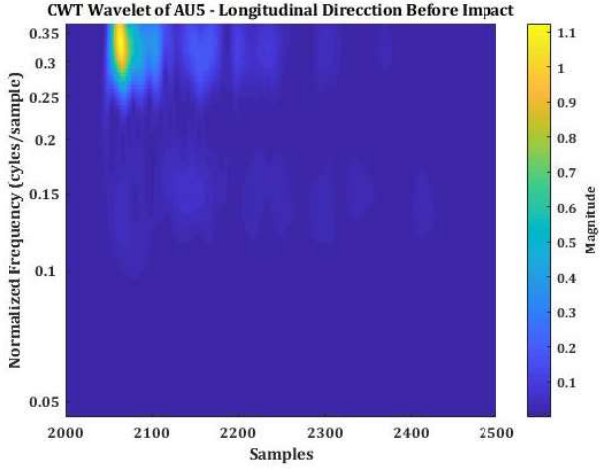
CWT Wavelet of AU5 - Longitudinal Direcction Before Impact
Normalized Frequency (cyles/sample)
0.35
0.3
0.25
0.2
0.15
0.1
0.05
2000
2100
2200
2300
2400
2500
Samples
Magnitude
1.1
1
0.9
0.8
0.7
0.6
0.5
0.4
0.3
0.2
0.1

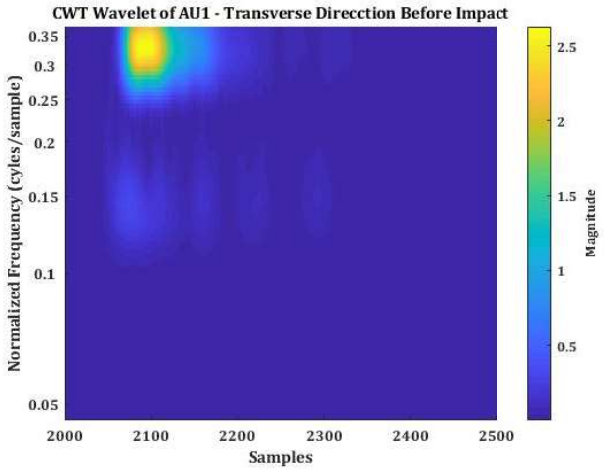
CWT Wavelet of AU1 - Transverse Direcction Before Impact
Normalized Frequency (cyles/sample)
0.35
0.3
0.25
0.2
0.15
0.1
0.05
2000
2100
2200
2300
2400
2500
Samples
Magnitude
2.5
2
1.5
1
0.5

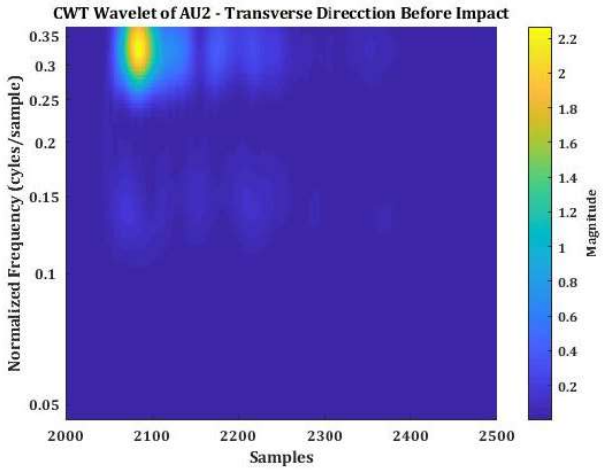
CWT Wavelet of AU2 - Transverse Direcction Before Impact
Normalized Frequency (cyles/sample)
0.35
0.3
0.25
0.2
0.15
0.1
0.05
2000
2100
2200
2300
2400
2500
Samples
Magnitude
2.2
2
1.8
1.6
1.4
1.2
1
0.8
0.6
0.4
0.2

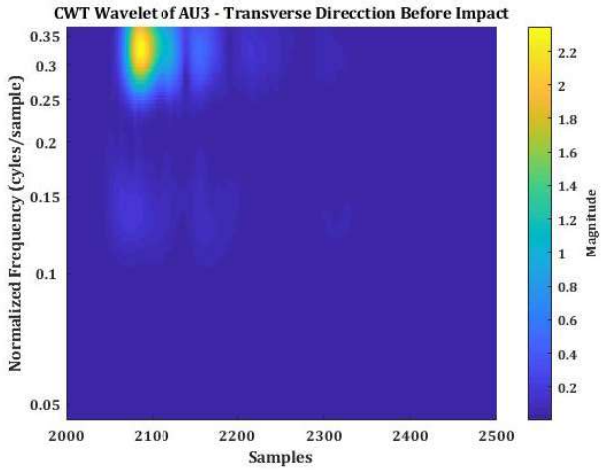
CWT Wavelet of AU3 - Transverse Direcction Before Impact
Normalized Frequency (cyles/sample)
0.35
0.3
0.25
0.2
0.15
0.1
0.05
2000
2100
2200
2300
2400
2500
Samples
Magnitude
2.2
2
1.8
1.6
1.4
1.2
1
0.8
0.6
0.4
0.2

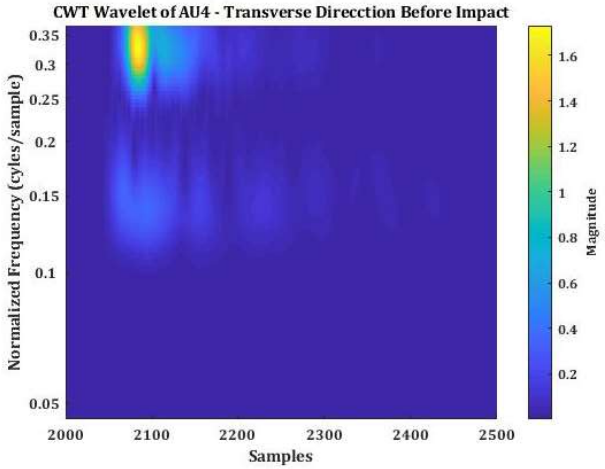
CWT Wavelet of AU4 - Transverse Direcction Before Impact
Normalized Frequency (cyles/sample)
0.35
0.3
0.25
0.2
0.15
0.1
0.05
2000
2100
2200
2300
2400
2500
Samples
Magnitude
1.6
1.4
1.2
1
0.8
0.6
0.4
0.2

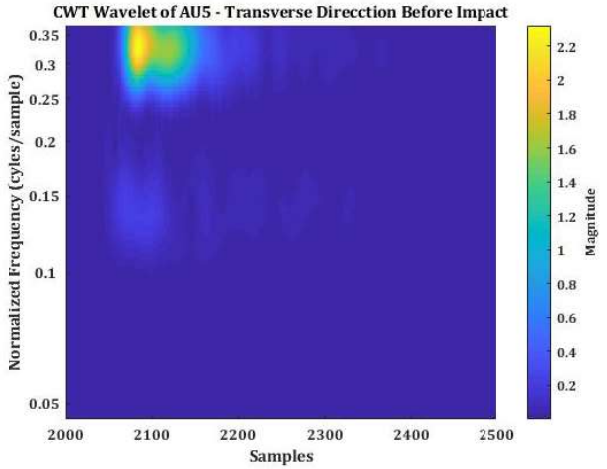
CWT Wavelet of AU5 - Transverse Direcction Before Impact
Normalized Frequency (cyles/sample)
0.35
0.3
0.25
0.2
0.15
0.1
0.05
2000
2100
2200
2300
2400
2500
Samples
Magnitude
2.2
2
1.8
1.6
1.4
1.2
1
0.8
0.6
0.4
0.2

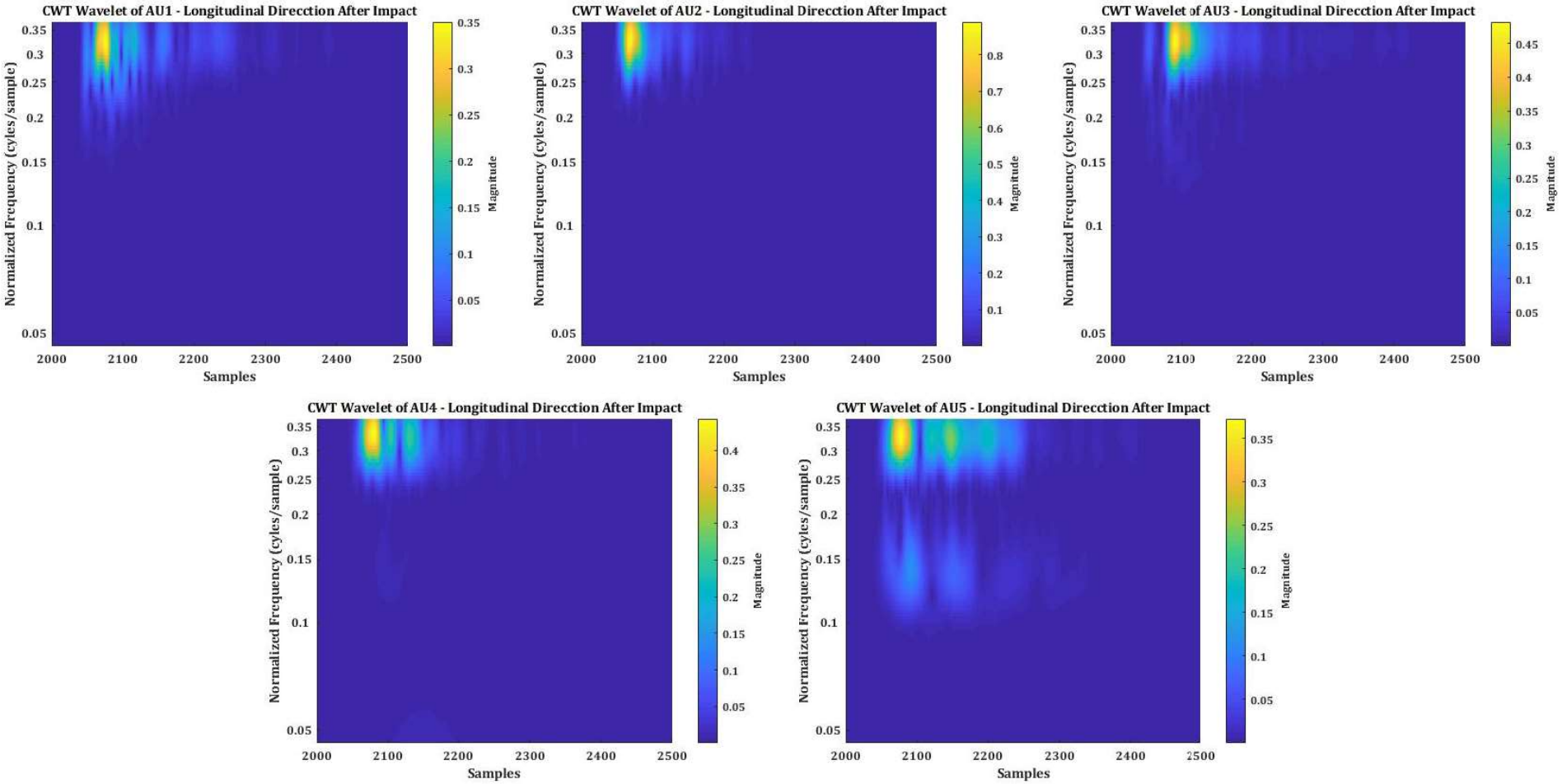
CWT Wavelet of AU1 - Longitudinal Direcction After Impact
CWT Wavelet of AU2 - Longitudinal Direcction After Impact
CWT Wavelet of AU3 - Longitudinal Direcction After Impact
CWT Wavelet of AU4 - Longitudinal Direcction After Impact
CWT Wavelet of AU5 - Longitudinal Direcction After Impact
Normalized Frequency (cyles/sample)
Samples
Magnitude

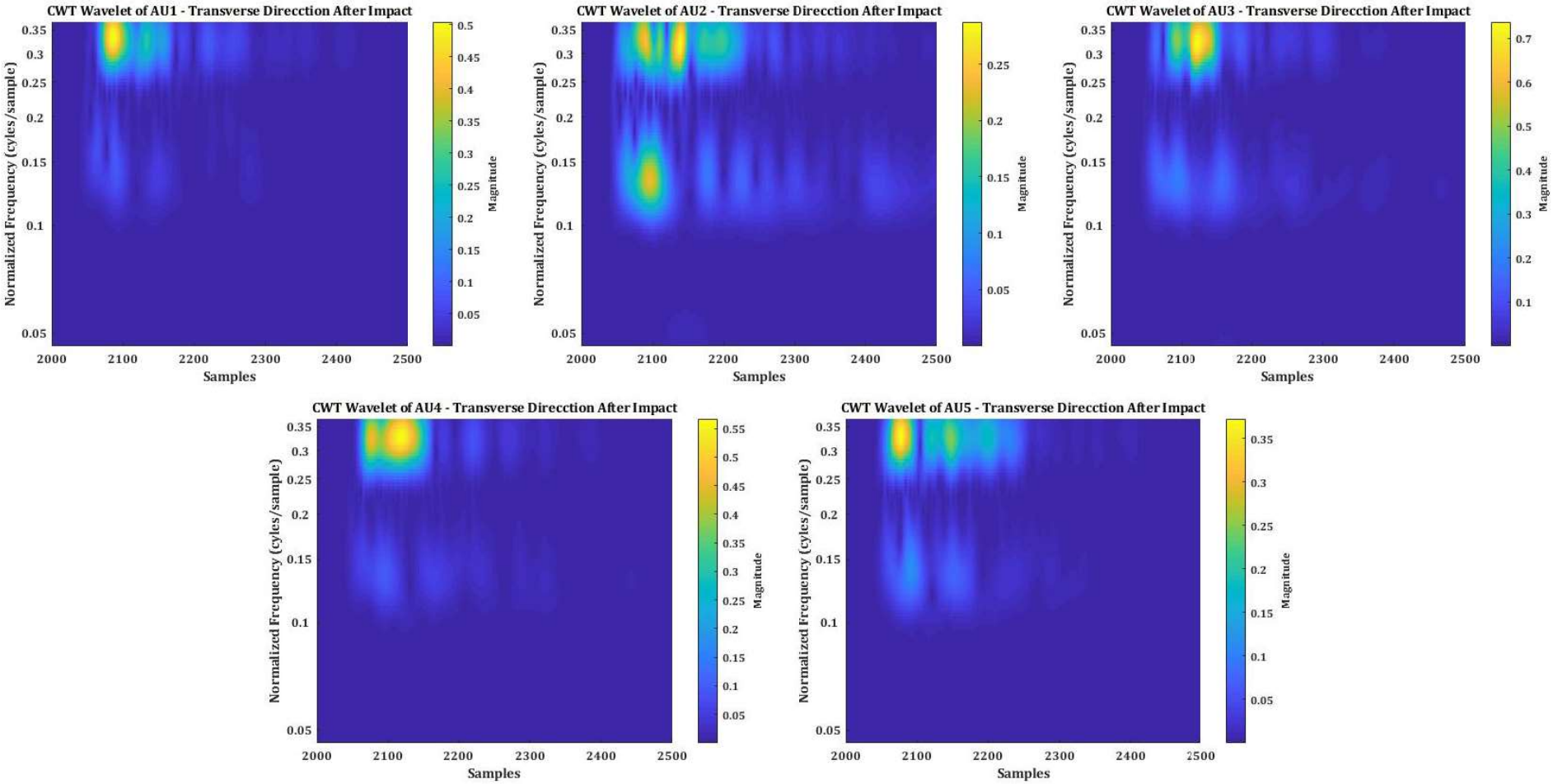
CWT Wavelet of AU1 - Transverse Direcction After Impact
CWT Wavelet of AU2 - Transverse Direcction After Impact
CWT Wavelet of AU3 - Transverse Direcction After Impact
CWT Wavelet of AU4 - Transverse Direcction After Impact
CWT Wavelet of AU5 - Transverse Direcction After Impact
Normalized Frequency (cyles/sample)
Samples
Magnitude

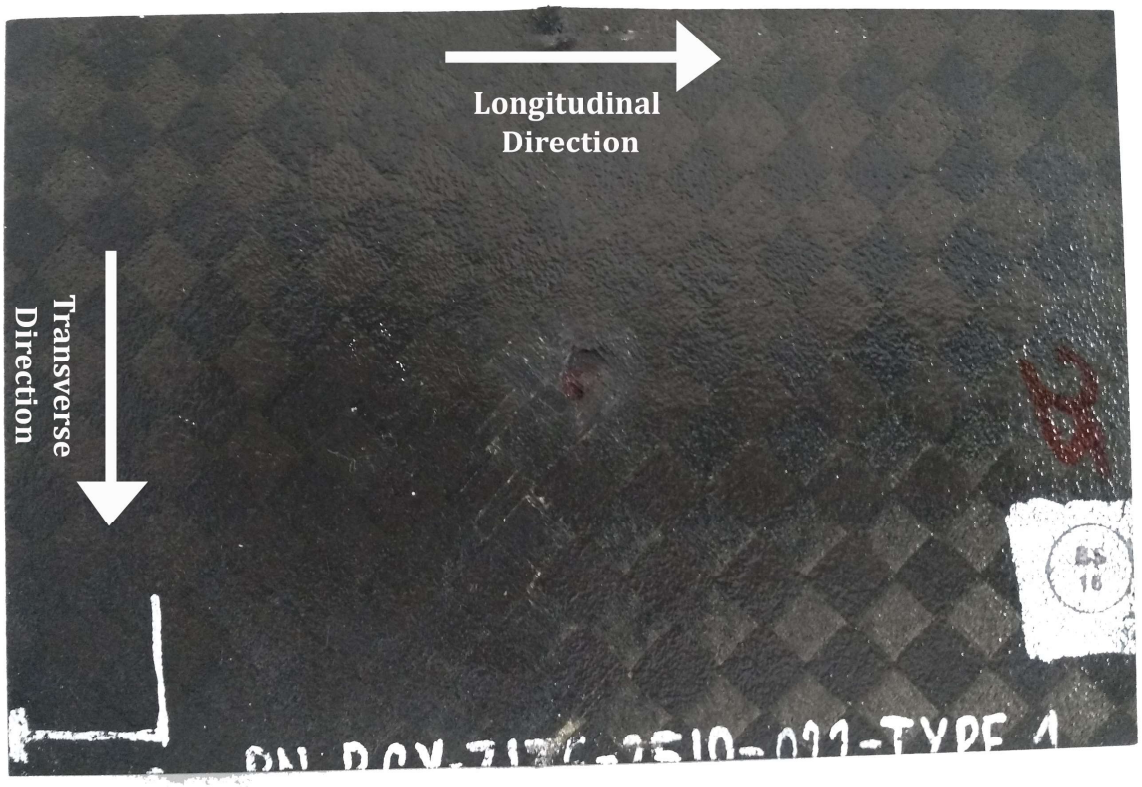
Longitudinal
Direction
Transverse
Direction

Table 1 – AE descriptors along longitudinal direction before the impact event

Specimen Denomination	**Signal Sent**				**Signal Received**			
	Amplitude *dB*	**Energy** *au*	**Duration** *ms*	**Count**	**Amplitude** *dB*	**Energy** *au*	**Duration** *ms*	**Count**
AU1	99	940.50	5443.40	82	80.50	61.20	798.30	137
AU2	99	934.10	5448.50	68	81.30	107.80	957.10	151
AU3	99	921.00	5440.30	60	84.10	104.10	1104.10	162
AU4	99	930.17	5444.67	73	81.33	71.00	922.83	142
AU5	99	944.20	5440.70	72	81.10	66.13	818.73	136

Table 2 – AE descriptors along transverse direction before impact event

Specimen Denomination	Signal Sent				Signal Received			
	Amplitude	Energy	Duration	Count	Amplitude	Energy	Duration	Count
	dB	*au*	*ms*		*dB*	*au*	*ms*	
AU1	99	961.60	5475.70	66	88.50	195.50	1317.30	1401
AU2	99	912.50	5446.40	70	86.40	142.00	1191.40	173
AU3	99	917.90	5441.10	75	87.20	135.90	1196.00	146
AU4	99	982.80	5455.10	61	85.50	104.80	1023.80	137
AU5	99	892.70	5424.90	63	86.50	169.80	1279.80	145

Table 3 – BVID residual indentation, Drop Weight Impact Test and CAI Test Results

Specimen Denomination	Residual Indention	Drop Weight Impact		CAI	
		Peak Force	Energy at Peak Force	CAI Force	CAI Strength
	mm	*N*	*J*	*kN*	*MPa*
AU1	-0.59	9849.16	26.84	110.52	1539.22
AU2	-0.41	11095.55	37.57	113.55	1581.42
AU3	-0.46	10652.33	36.23	111.56	1553.74
AU4	-0.39	10393.53	47.72	119.80	1668.58
AU5	-1.74	9090.62	32.20	104.90	1461.02

Table 4 – AE descriptors along longitudinal direction after impact event

Specimen Denomination	Signal Sent				Signal Received			
	Amplitude *dB*	Energy *au*	Duration *ms*	Count	Amplitude *dB*	Energy *au*	Duration *ms*	Count
AU1	99	964.50	5476.60	71	71.00	20.10	411.40	96
AU2	99	898.10	5418.80	58	79.10	43.50	401.20	105
AU3	99	958.88	5433.50	53	72.63	26.50	436.88	113
AU4	99	970.70	5466.70	65	72.20	27.10	429.20	97
AU5	99	954.90	5439.40	58	70.90	25.10	445.20	98

Table 5 – AE descriptors along transverse direction after impact event

Specimen Denomination	Signal Sent				Signal Received			
	Amplitude	Energy	Duration	Count	Amplitude	Energy	Duration	Count
	dB	*au*	*ms*		*dB*	*au*	*ms*	
AU1	99	936.60	5445.30	71	73.50	36.20	583.80	126
AU2	99	917.00	5431.20	72	75.00	48.00	799.30	120
AU3	99	919.50	5441.20	64	77.00	112.10	541.50	123
AU4	99	940.00	5442.00	68	74.75	50.38	689.63	113
AU5	99	965.20	5465.20	74	70.60	34.20	439.20	108